Low-energy properties of the ferromagnetic metallic phase in manganites: Slave-fermion approach to the quantum double-exchange model

Yu-Li Lee
Physics Department, National Changhua University of Education, Changhua, Taiwan, Republic of China

Yu-Wen Lee
Physics Department, Tunghai University, Taichung, Taiwan, Republic of China
(Received 21 September 2006; published 9 February 2007)

We study the low-energy properties of the one-orbital quantum double-exchange model by using the slave fermion formulation. We construct a mean-field theory which gives a simple explanation for the magnetic and thermodynamic properties of the ferromagnetic metallic phase in manganites at low energy. The resulting electron spectral function and tunneling density of states show an incoherent asymmetric peak with weak temperature dependence, in addition to a quasiparticle peak. We also show that the gauge fluctuations in the ferromagnetic metallic phase are completely screened due to the Anderson-Higgs mechanism. Therefore, the mean-field state is robust against gauge fluctuations and exhibits spin-charge separation at low energy.

DOI: 10.1103/PhysRevB.75.064411 PACS number(s): 75.47.Lx, 75.10.Lp, 79.60.−i

I. INTRODUCTION

The phenomenon of colossal magnetoresistance (CMR) is known to occur in various doped perovskite manganese oxides with the chemical formula $Re_{1-x}A_xMnO_3$, where Re is the rare earth such as La or Nd and A is a divalent alkali such as Sr or Ca.[1] More recent studies revealed a complex phase diagram and very rich physics.[2] Therefore, it is of great theoretical interest to find a proper minimal model for these CMR systems, which can account for the important common features, such as the transport and magnetic properties, shared by all these materials, while leaving out many non-universal peculiarities due to crystal environment and atomic structure of individual compounds.

One of the universally recognized common feature of these CMR compounds is the sizable ferromagnetic (FM) Hund's rule coupling J_H between the core spins and those of the e_g electrons. This gives the double-exchange (DE) interaction[3–7] which is believed to be a fundamental mechanism in explaining many of the interesting features of the CMR compounds. From this point of view, a usual starting point to analyze the properties of the CMR material is the standard DE Hamiltonian, supplemented with other terms, such as the Hubbard repulsion U, the antiferromagnetic (AF) superexchange interactions between core spins J_{AF}, etc. For the case of CMR manganites, band theory calculations[8] suggest the typical values of the hopping amplitude $t \sim 0.3-0.5$ eV, $J_H \sim 2.5$ eV, and $U \sim 6-8$ eV.

Motivated by experimental findings, there has been significant progress in the study of the DE Hamiltonian, notably applying the Schwinger boson[9,10] or $1/S_c$ expansion.[11,12] ($S_c = 3/2$ is the core spin.) Most of these approaches lead to a simple Fermi liquid (a doped band insulator) picture for the ground state of the FM metallic phase, which cannot fully explain the results of experiments, especially the optical conductivity at low energy[13,14] and the angle-resolved photoemission (ARPES) measurements.[15–17] Recently, Golosov tried to address parts of the discrepancy by including the on-site Coulomb repulsion through the Hartree-Fock approximation.[18] Although some interesting results were found, the Hartree-Fock approximation is still based on the Fermi-liquid picture. To capture the low-energy physics for large values of U and J_H properly, a slave-fermion approach has been proposed.[10,19] A recent work by Hu[20] along this direction has shown that the massless fluctuations of the longitudinal part of the gauge fields arising from the slave-fermion approach indeed dramatically change the behavior of the spectral function of e_g electrons at low energy.

The purpose of the present paper is to give a simple mean-field description on the low-temperature properties of the DE system in the large U, J_H limit. (For the implementation of the large U, J_H limit, see Sec. II.) Orbital fluctuations, Jahn-Teller effect, and nanoscale phase separation, though very interesting, make analysis difficult. Therefore, we shall focus our attention on the region where the DE mechanism is the dominant factor, namely, the region at the hole concentration $0.2 < x < 0.5$ and away from the critical temperature T_c. We propose a mean-field theory based on the slave-fermion scheme, which exhibits spin-charge separation at low energy, and use it to calculate various low-energy properties in the FM metallic phase. Among them, the most important result is that the quasiparticle peak in the electron spectral function is reduced at low temperatures and the spectral weight is transferred to an asymmetric broad peak away from the Fermi surface, which is a natural consequence of the spin-charge separation in our theory. The other physical properties in the FM metallic phase we have studied are as follows: (i) The magnon dispersion at the mean-field level is similar to that of a simple cubic Heisenberg ferromagnet, which has been verified by inelastic neutron scattering measurements. (ii) The magnitudes of the spin stiffness at $T=0$ and the coefficients in the low-temperature specific heat, obtained from the mean-field theory, are consistent with experimental data. (iii) The structure of the optical conductivity at low energy is of the form similar to that observed by experiments, and the Drude weight is reduced.

We now briefly outline the structure of our paper. In Sec. II, we will introduce the quantum double-exchange (QDE) model and develop a slave-fermion mean-field theory. The results of the mean-field theory is presented in Sec. III. We will show the stability of our mean-field state against the gauge fluctuations in Sec. IV. The last section is devoted to a conclusive discussion.

II. THE MODEL AND THE SLAVE-FERMION MEAN-FIELD THEORY

We shall start with the quantum double-exchange (QDE) model described by the following Hamiltonian:[19]

$$H = -t\sum_{i,u,\sigma}(\bar{c}^{\dagger}_{i+u\sigma}\bar{c}_{i\sigma} + \text{H.c.}) - J_H\sum_{i} \boldsymbol{S}^c_i \cdot \boldsymbol{s}_i, \tag{1}$$

where the first and second terms describe electronic hopping and DE couplings, respectively. Here, $\boldsymbol{S}^c$ denotes the core spin, $\boldsymbol{s}$ is the spin operator of e_g electrons, $\boldsymbol{u}$ is a unit vector connecting the nearest-neighbor sites around site $\boldsymbol{i}$ (for a simple cubic lattice, $\boldsymbol{u}=\hat{\boldsymbol{x}}$, $\hat{\boldsymbol{y}}$, and $\hat{\boldsymbol{z}}$), and $\bar{c}_{i\sigma}$ is the annihilation operator of e_g electrons at site $\boldsymbol{i}$ with spin σ. In Eq. (1), we have neglected the superexchange interactions between core spins. This is because $J_{\text{AF}}\sim 5-10$ meV in manganites, which is much smaller than t. Moreover, in the undoped compounds, a Jahn-Teller distortion lifts the orbital degeneracy of the e_g electrons with the energy scale $E_{\text{JT}} \sim 1-1.6$ eV. Thus, to study the low-energy physics in the hole-doped region ($x<0.5$), one may in a first approximation ignore the orbital degeneracy and apply the one-orbital model. To take into account the fact that the on-site Coulomb interactions between e_g electrons is the largest energy scale in manganites, we impose the no-double-occupancy (NDO) condition on the e_g electron operators,

$$n_i \equiv \sum_{\sigma} \bar{c}^{\dagger}_{i\sigma}\bar{c}_{i\sigma} = 0,1. \tag{2}$$

Therefore, $\bar{c}_{i\sigma}$ and $\bar{c}^{\dagger}_{i\sigma}$ cannot obey the canonical anticommutation relations, and Eq. (1) is valid for energies much lower than U.

Because of the NDO condition [Eq. (2)], the system becomes a strongly correlated one. One popular way to solve this kind of problems is to introduce a pair of slave fields to rewrite the $\bar{c}$ operator. Here we adopt the slave-fermion representation,

$$\bar{c}_{i\sigma} = f^{\dagger}_i b_{i\sigma}, \tag{3}$$

where f_i and $f^{\dagger}_i$ satisfy the canonical anticommutation relations, and $b_{i\sigma}$ and $b^{\dagger}_{i\sigma}$ satisfy the canonical commutation relations.[21] In this way, the charge and spin degrees of freedom of e_g electrons are represented by f (holon) and b (spinon) fields, respectively. In terms of f_i and $b_{i\sigma}$, the NDO condition becomes an identity

$$\sum_{\sigma} b^{\dagger}_{i\sigma}b_{i\sigma} + f^{\dagger}_i f_i = 1. \tag{4}$$

In manganites, one may further simplify Eq. (1). Since $J_H \sim 10t$, at the energy scale much lower than J_H, it suffices to consider the Hilbert space in which the e_g electron spin is parallel to the core spin. One may introduce another Schwinger bosons $d_{i\sigma}$ and $d^{\dagger}_{i\sigma}$ to describe the total spin. Within this subspace, it can be shown that the b field is associated with the d field through the relation[10,19]

$$b_{i\sigma} = \frac{1}{\sqrt{2S}} d_{i\sigma}, \tag{5}$$

with $S=2$. Collecting the above results, in the limit $J_H/t \to +\infty$, Eq. (1) is reduced to the one

$$H_{\text{DE}} = -t\sum_{i,u,\sigma}(\bar{c}^{\dagger}_{i+u\sigma}\bar{c}_{i\sigma} + \text{H.c.}), \tag{6}$$

and the NDO condition becomes

$$\sum_{\sigma} d^{\dagger}_{i\sigma}d_{i\sigma} + f^{\dagger}_i f_i = 2S. \tag{7}$$

We shall take Eq. (6) as a minimal model to describe the FM metallic phase in manganites.[22]

To proceed, we turn into the path-integral formalism. The partition function of the QDE model in the large J_H limit can be written as

$$Z = \int D[f^{\dagger}]D[f]D[d^{\dagger}_{\sigma}]D[d_{\sigma}]D[\lambda]\exp\left\{-\int_0^{\beta} d\tau \sum_i L\right\}, \tag{8}$$

where

$$L = \sum_{\sigma} d^{\dagger}_{i\sigma}(\partial_\tau + \lambda_i)d_{i\sigma} + f^{\dagger}_i(\partial_\tau + i\lambda_i - \mu_0)f_i + \frac{t}{2S}\sum_{u,\sigma}(f^{\dagger}_{i+u}f_i d^{\dagger}_{i\sigma}d_{i+u\sigma} + \text{H.c.}) - 2iS\lambda_i,$$

μ_0 is the chemical potential of holes, and λ_i is the Lagrangian multiplier to impose the NDO condition. To facilitate the mean-field analysis, one may perform the Hubbard-Stratonovich transformation to decouple the hopping term, and the Lagrangian becomes

$$\begin{aligned} L = {} & \sum_{\sigma} d^{\dagger}_{i\sigma}(\partial_\tau + i\lambda_i)d_{i\sigma} + f^{\dagger}_i(\partial_\tau + i\lambda_i - \mu_0)f_i \\ & - \frac{t}{2S}\sum_{u}(\chi^{\dagger}_{i+u,i}f^{\dagger}_{i+u}f_i + \text{H.c.}) - \frac{t}{2S}\sum_{u,\sigma}(\eta^{\dagger}_{i+u,i}d^{\dagger}_{i+u\sigma}d_{i\sigma} + \text{H.c.}) \\ & - \frac{t}{S}\sum_{u}(\eta^{\dagger}_{i+u,i}\chi_{i+u,i} + \text{H.c.}) - 2iS\lambda_i. \end{aligned} \tag{9}$$

We notice that there is a U(1) gauge structure in the slave-fermion scheme, which is reflected in the invariance of L (up to a total derivative in τ) under the U(1) gauge transformation,

$$\begin{aligned} & f_i \to f_i e^{-iw_i}, \quad d_{i\sigma} \to d_{i\sigma}e^{-iw_i}, \\ & \chi_{i+u,i} \to \chi_{i+u,i}e^{i(w_{i+u}-w_i)}, \\ & \eta_{i+u,i} \to \eta_{i+u,i}e^{i(w_{i+u}-w_i)}, \\ & \lambda_i \to \lambda_i + \partial_\tau w_i. \end{aligned} \tag{10}$$

Motivated by the DE mechanism, which allows the coherent hopping of charge carriers in a FM background, we consider the following mean-field ansatz:

$$\chi_{i+u,i} = \chi, \quad \eta_{i+u,i} = \eta, \quad i\lambda_i = \Delta, \tag{11}$$

where χ, η, and Δ are real. Inserting Eq. (11) into Eq. (9), the mean-field Lagrangian can be written as

$$L_{\rm mf} = \sum_{\sigma} d_{i\sigma}^{\dagger}(\partial_\tau + \Delta)d_{i\sigma} + f_i^{\dagger}(\partial_\tau + \Delta - \mu_0)f_i - \frac{\chi t}{2S}\sum_{u}(f_{i+u}^{\dagger}f_i + \text{H.c.}) - \frac{\eta t}{2S}\sum_{u,\sigma}(d_{i+u\sigma}^{\dagger}d_{i\sigma} + \text{H.c.}) - \frac{zt}{S}\eta\chi - 2S\Delta,$$

where $z=6$ is the coordination number. Now $L_{\rm mf}$ becomes quadratic in f and d_σ, and one may integrate them out to obtain the mean-field grand potential. The mean-field equations are obtained through minimizing the mean-field grand potential with respect to the mean-field parameters, yielding

$$\frac{1}{N}\sum_{k} n_B(\epsilon_{bk} + \Delta) = S - \frac{x}{2}, \tag{12}$$

$$\frac{1}{N}\sum_{k} \epsilon_{fk} n_F(\epsilon_{fk} - \mu_f) = \frac{zt}{S}\chi\eta, \tag{13}$$

$$\frac{1}{N}\sum_{k} \epsilon_{bk} n_B(\epsilon_{bk} + \Delta) = \frac{zt}{2S}\chi\eta, \tag{14}$$

where $n_F(x)=(e^{\beta x}+1)^{-1}$ is the Fermi-Dirac distribution, $n_B(x)=(e^{\beta x}-1)^{-1}$ is the Bose-Einstein distribution, N is the number of lattice points, $\epsilon_{fk}=-\frac{\chi t}{S}\sum_{u}\cos(\boldsymbol{k}\cdot\boldsymbol{u})$, and $\epsilon_{bk}=-\frac{\eta t}{S}\sum_{u}\cos(\boldsymbol{k}\cdot\boldsymbol{u})$. The chemical potential of holons, $\mu_f=\mu_0-\Delta$, is associated with the hole concentration x through the equation

$$\frac{1}{N}\sum_{k} n_F(\epsilon_{fk} - \mu_f) = x. \tag{15}$$

Equations (12)–(15) are the mean-field equations we want to solve.

Before solving these mean-field equations numerically, we may look into the physics revealed by them. Equation (12) is nothing but the number equation of free bosons with the average number of particles per site $S-x/2$ and the chemical potential $-\Delta$. In three dimensions, there exists a critical temperature $T_c>0$ so that $\Delta=\Delta_0$ for $T\leqslant T_c$ and $\Delta>\Delta_0$ for $T>T_c$, where $\Delta_0=\eta zt/(2S)$ is the bottom of the spinon band ϵ_{bk}. When $\Delta=\Delta_0$, the Bose-Einstein condensation (BEC) of the d bosons occurs, which corresponds to the FM phase. On the other hand, it is the paramagnetic (PM) phase for $\Delta>\Delta_0$. In this scenario, the PM to FM phase transition in manganites is associated with the BEC of the d bosons, and T_c corresponds to the Curie temperature.

With the above understanding in mind, we can see that deep inside the FM phase, without loss of generality, one may choose the direction of magnetization to be the z axis and set $\langle d_{i\uparrow}\rangle=\sqrt{2S-x}$ and $\langle d_{i\downarrow}\rangle=0$ in terms of a proper spin SU(2) rotation. (This parametrization for d bosons is consistent with the experiment which shows the complete spin polarization of conduction electrons in manganites.[23]) Further, for $T\ll T_c$, one may neglect the amplitude fluctuations of $d_{i\uparrow}$. As for the phase fluctuations of $d_{i\uparrow}$, it can be absorbed into $d_{i\downarrow}$ and f_i by choosing a particular gauge or performing a proper U(1) gauge transformation with the help of the U(1) gauge invariance of L. Thus, to obtain the low-energy effective Hamiltonian in the FM phase, it suffices to set

$$d_{i\uparrow} = \sqrt{2S-x}, \quad d_{i\downarrow} = b_i, \tag{16}$$

in $L_{\rm mf}$. On account of the condensation of the d bosons, it turns out that the gauge fluctuations acquire a finite energy gap through the Anderson-Higgs mechanism, so that the mean-field state is stable against the gauge fluctuations. As a result, the physics in the FM phase at energies much lower than the gap of gauge bosons, E_g, can be described by the following effective Hamiltonian in the grand canonical ensemble:

$$H_{\rm FM} = \sum_{k}[(\epsilon_k - \mu_f)f_k^{\dagger}f_k + \omega_k b_k^{\dagger}b_k], \tag{17}$$

where $f_i=\frac{1}{\sqrt{N}}\sum_k e^{i\boldsymbol{k}\cdot\boldsymbol{i}}f_k$ and $b_i=\frac{1}{\sqrt{N}}\sum_k e^{i\boldsymbol{k}\cdot\boldsymbol{i}}b_k$. (For the details of the derivation, see Sec. IV.) The f field describes the spinless charged excitations—holons, with the dispersion relation

$$\epsilon_k = \left(1 - \frac{x}{4}\right)t\sum_{u}\cos(\boldsymbol{k}\cdot\boldsymbol{u}), \tag{18}$$

and we shall see that the b field describes the FM spin waves—magnons, with the dispersion relation

$$\omega_k = \frac{\eta t}{2}\left(3 - \sum_{u}\cos(\boldsymbol{k}\cdot\boldsymbol{u})\right). \tag{19}$$

In Eq. (17), we have neglected the interactions between holons and magnons, which are irrelevant operators in the sense of the renormalization group (RG). Equation (17) indicates that there is spin-charge separation at low energy in the FM metallic phase. (We will come back to this point in Sec. IV.) Further, we shall see later that the bandwidth of holons is of the order of t, while that of magnons is of the order of $0.1t$.

III. RESULTS IN THE FERROMAGNETIC METALLIC PHASE

A. Magnetic properties

(a) Magnon dispersion. We shall first employ our mean-field theory to calculate the transverse spin-spin correlation function, which is defined as

$$i\mathcal{S}_\perp(t,\boldsymbol{x}) \equiv \Theta(t)\langle[S_i^{+}(t),S_j^{-}(0)]\rangle, \tag{20}$$

where $S_i^{\pm}=S_i^x \pm iS_i^y$ and $\boldsymbol{x}=\boldsymbol{i}-\boldsymbol{j}$. In the large J_H limit, $S_\pm$ can be expressed by the d bosons

$$S_i^{+} = d_{i\uparrow}^{\dagger}d_{i\downarrow}, \quad S_i^{-} = d_{i\downarrow}^{\dagger}d_{i\uparrow}. \tag{21}$$

The Fourier transform of $\mathcal{S}_\perp(t,\boldsymbol{x})$, denoted by $\mathcal{S}_\perp(\omega,\boldsymbol{q})$, can be obtained from the corresponding Matsubara function

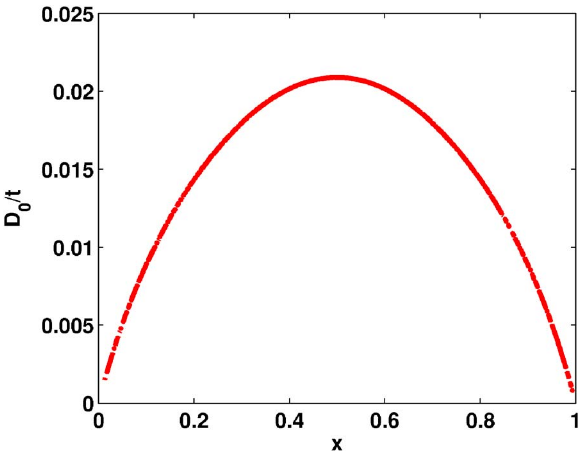

FIG. 1. (Color online) The doping dependence of the spin stiffness at $T=0$. Here we set the lattice constant $l=1$.

through analytical continuation. In the FM phase, $\mathcal{S}_{\perp}(\omega,\boldsymbol{q})$ can be related to the two-point correlation function of the b field within the mean-field theory,

$$\mathcal{S}_{\perp}(\omega,\boldsymbol{q}) \approx x_d(T) S^T(\omega,\boldsymbol{q}), \tag{22}$$

where $x_d(T)=\langle d^{\dagger}_{\boldsymbol{i}\uparrow} d_{\boldsymbol{i}\uparrow}\rangle$ is the average number of d bosons in the condensate per site at temperature T and $S^T(\omega,\boldsymbol{q})$ is the Fourier transform of the retarded Green function of the b field. In view of Eq. (22), one may identify the excitations corresponding to the b field as the magnons.

We notice that the form of the magnon dispersion we obtained [Eq. (19)] is identical to that given by the FM Heisenberg model on a simple cubic lattice with nearest-neighbor interactions only. This result is similar to that predicted by previous studies on the DE model.[3–7] However, within the present framework, the Heisenberg-type behavior for the magnon dispersion is a mean-field result. By taking into account the so far ignored irrelevant (in the sense of the RG) interactions between magnons, a deviation from the Heisenberg spectrum is expected. On the general ground of the RG, we expect that the deviation from the mean-field result (the Heisenberg spectrum) will become more noticeable away from the zone center. Furthermore, the small values of the spin stiffness at $T=0$ in the regions $x\to 0$ and $x\to 1$ (see Fig. 1) suggest that the mean-field results may receive considerable corrections in these regions. On the other hand, for the physically interested doping regime $0.2<x<0.5$, the mean-field results should be robust. Recent works on the DE model, such as the spin-wave theory based on the large S_c expansion[11,12] and an exact calculation on a finite ring[24] in the limit $J_H/t \gg 1$, have revealed a deviation of the magnon dispersion from the Heisenberg spectrum in the DE model. The deviation is prominent at large momenta,[11,24] and the overall deviation is very small in the doping range $0.2<x<0.6$.[24] Our theory is consistent with these results.

A Heisenberg-type behavior for the magnon dispersion may provide a reasonably accurate picture for manganese oxides with large values of T_c.[25] However, recent experiments indicate deviations from this canonical behavior in compounds with lower values of T_c. In particular, the softening of the mangon dispersion near the boundary of the Brillouin zone is observed.[26] Such an issue clearly depends on the details of the short-distance physics, and is beyond the scope of the present work. A systematic calculation which incorporates the magnon-magnon and magnon-holon interactions, such as those given by Eq. (47), may be helpful.[27] However, for a complete comparison with experimental data, additional ingredients, such as orbital fluctuations and orbital-lattice couplings, may also need to be taken into account.[10]

A finite damping rate of magnons at $T=0$ in the DE model has been pointed out in Refs. 11, 12, and 28. To address this problem within the slave-fermion theory, we must go beyond the mean-field results. In fact, the magnon acquires a finite lifetime, even at $T=0$, at the two-loop order of the magnon self-energy diagrams by taking into account the interactions between holons and magnons. [The leading terms of these interactions are given by Eq. (47).] The physical origin of a nonvanishing $T=0$ damping rate of magnons can be easily understood based on our spin-charge separated mean-field state: Because the magnon dispersion, which is proportional to k^2 near the zone center, is definitely immersed into the "particle-hole" continuum of holons in three dimensions, the magnon can decay by exciting a single "particle-hole" pair and another magnon, which is similar to the physics of Landau damping in the Fermi liquids.[29] Since the interactions between holons and magnons are irrelevant operators in the sense of the RG, we expect that the damping rate of the magnon near the zone center ($k=0$) is, at least, proportional to k^{α} with $\alpha \geqslant 4$ in three dimensions by the power counting usually employed in the momentum-space RG. (Additional on-shell constraints may further increase the value of α.) The spin-wave theory in the $J_H/t \to +\infty$ limit predicts that the damping rate of the magnon near the zone center is proportional to k^6 in three dimensions,[11,12] which implies that it is indeed due to the irrelevant interactions. A full calculation by incorporating these irrelevant operators is beyond the scope of this paper, and their effects within the present framework are reserved for further studies.

(b) Doping dependence of the spin stiffness at $T=0$. From Eq. (19), the magnon dispersion in the long wavelength limit $\boldsymbol{k}\to 0$ is given by $\omega_{\boldsymbol{k}} \approx D_0 \boldsymbol{k}^2$ where

$$D_0 = \frac{\eta t l^2}{2S}, \tag{23}$$

is the spin stiffness at $T=0$ and l is the lattice constant. Thus, the doping dependence of D_0 can be extracted from that of η. The result is shown in Fig. 1.

Our theory predicts that D_0 is symmetric in x with respect to the quarter-filling $x=0.5$. This result is similar to that predicted by the spin-wave theory of the DE model in the limits $J_H/t \to +\infty$ and $S_c \to +\infty$,[11] except that the magnitude of $D_0(x)$ around $x=0.5$ we obtained is smaller. The values of D_0 we obtained are $D_0/(tl^2)=0.0144, 0.018, 0.0202$ for $x=0.2, 0.3, 0.4$. Using the relation $D_0=JS_{\text{eff}}l^2$, where $S_{\text{eff}}=2-x/2$ is the average spin for each site and J denotes the effective exchange coupling between spins, one may get $J=0.0076t$, $0.0097t, 0.0112t$ for $x=0.2, 0.3, 0.4$, which correspond to J

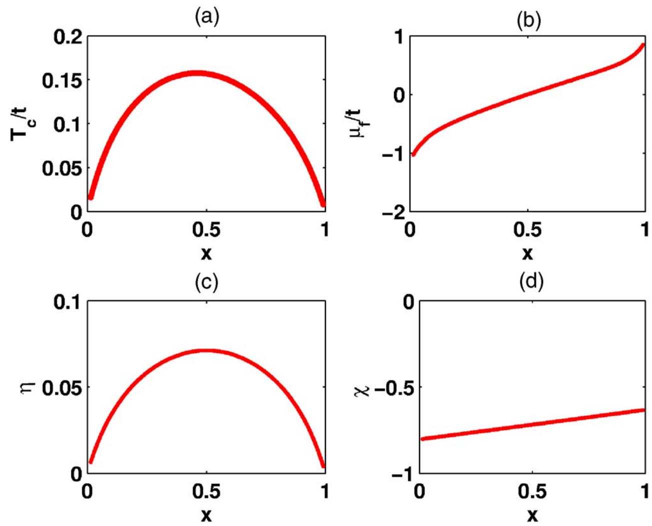

FIG. 2. (Color online) (a) T_c/t vs x; (b) μ_f/t vs x at $T=T_c$; (c) η vs x at $T=T_c$; (d) χ vs x at $T=T_c$.

$=2.28, 2.91, 3.36$ meV if we use $t=0.3$ eV, $J\approx 1.9, 2.4$ meV found in $La_{0.8}Sr_{0.2}MnO_3$ (Ref. 25) and $La_{0.7}Pb_{0.3}MnO_3$,[31] respectively. We see that the values of J we obtained are consistent with those extracted from experimental data. To sum up, for the magnon dispersion relation, the difference between our mean-field theory and the spin-wave theory of the DE model in the doping range $0.2<x<0.5$ mainly lies at the doping dependence of the spin stiffness at $T=0$ and its magnitude.

Finally, we mention that the low-temperature magnetization in the FM phase can be easily calculated within the present mean-field theory, and it is

$$M(T) = M_0\left[1 - \frac{\zeta(3/2)}{M_0}\left(\frac{T}{4\pi D_0}\right)^{3/2} + \cdots\right], \tag{24}$$

which is identical to that predicted by the simple-cubic Heisenberg ferromagnet, where $M_0=(2-x/2)l^{-3}$ is the magnetization at $T=0$.

B. Estimation of T_c

Next, we would like to estimate T_c within our mean-field theory, which can be obtained from the mean-field equations [Eqs. (12)–(15)] numerically by setting $\Delta=\Delta_0$. The numerical results are shown in Fig. 2. A few points about our results should be discussed. First of all, T_c is asymmetric in x with respect to the point $x=0.5$ though $\eta(T_c)$ is still symmetric in x with respect to $x=0.5$. This is in contrast to D_0. This asymmetry suggests that the FM phase is more robust at $x<0.5$ by including strong on-site Coulomb repulsions and Hund's rule couplings properly. Next, the previous work based on the dynamical mean-field theory gives an estimate of T_c for $J_H/t\gg 1$: $T_c/t=0.146$ at $x=0.3$.[7] Our mean-field theory predicts $T_c/t=0.1454$ at $x=0.3$, which is quite close to the value obtained from the dynamical mean-field theory. Finally, the maximum of T_c/t is reached at $x=0.458$ with the value $T_c/t=0.1575$, which corresponds to $T_c\sim 548$ K for $t\sim 0.3$ eV. This value is about 2 times of that obtained by experiments. As usual, the fluctuations will reduce the mean-field value. Nevertheless, the difference between the mean-field result and experimental data may still not be explained even if we include the fluctuations. This may not be surprising since, after all, T_c is a nonuniversal quantity and the above result simply indicates that to have a good estimation of T_c a few ingredients that are ignored in the QDE model, such as the AF superexchange interactions between core spins, orbital fluctuations, and electron-phonon interactions, must be included. In fact, experiments on the oxygen-isotope substitution show that phonons are important in the determination of T_c.[30]

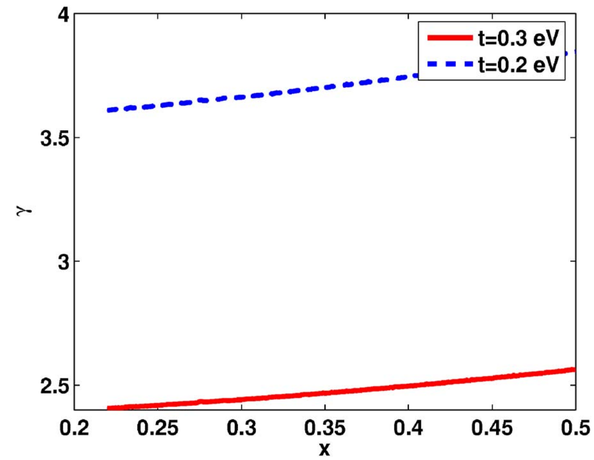

FIG. 3. (Color online) $\gamma=c_{elec}/T$, in unit of $mJ/mol\,K^2$, in the doping range $0.2<x<0.5$.

C. The low-temperature specific heat

Low-temperature ($T\leq 10$ K) heat-capacity measurements provide information regarding the bulk properties of solids. For a magnetic solid, the low-temperature specific heat is composed of numerous contributions and it is typically given by

$$c_v = c_{elec} + c_{hyp} + c_{lat} + c_{mag}. \tag{25}$$

Here c_{elec} is the electronic contribution, which takes the form $c_{elec}=\gamma T$, c_{hyp} arises from the hyperfine field of the nuclear moment, c_{lat} is the contribution of phonons, and c_{mag} is the contribution from the magnetic spin waves, which is usually estimated as the form $\sum_n B_n T^n$.

In our theory, c_{elec} is primarily given by the holon sector due to the spin-charge separation at low energy, yielding

$$\gamma = \frac{(\pi k_B)^2}{3} g(\epsilon_F),$$

away from the van Hove singularities, where k_B is the Boltzmann constant, and $g(\epsilon_F)$ is the density of states (DOS) of holons at the Fermi energy.

Figure 3 shows the values of γ in the doping range $0.2<x<0.5$ with $t=0.3$ eV (solid line) and $t=0.2$ eV (dashed line). The magnitudes of γ we obtained are consistent with

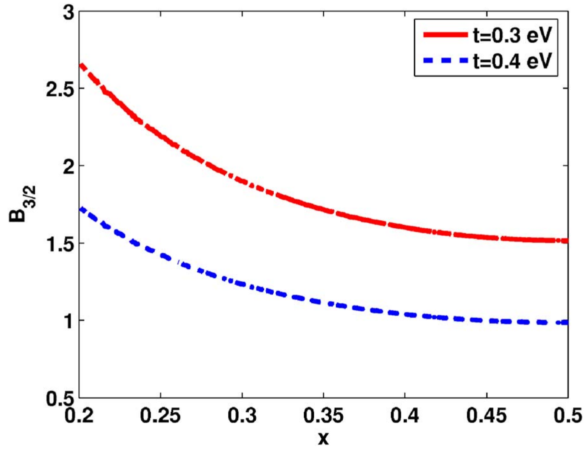

FIG. 4. (Color online) $B_{3/2}=c_{\mathrm{mag}}/T^{3/2}$, in unit of mJ/mol $K^{5/2}$, in the doping range $0.2<x<0.5$.

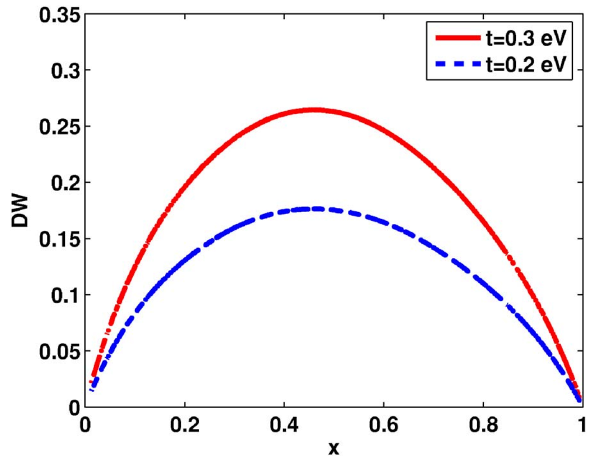

FIG. 5. (Color online) DW as a function of x.

the experimental data. Furthermore, the mean-field theory predicts a very weak doping dependence of γ, which is approximately given by

$$\gamma \propto \frac{1}{1-x/4}. \tag{26}$$

Such a weak doping dependence of γ may not contradict to the experimental data at $x=0.2$ and 0.3, where the measured values of γ ($\approx$3.3 mJ/mol K^2) appear to be nearly a constant in the FM metallic phase.[31] More detailed experiments is warranted to resolve this issue.

As for c_{mag}, the magnon contribution to the low-temperature specific heat is similar to that in the simple-cubic Heisenberg ferromagnet and takes the form

$$c_{\mathrm{mag}} = B_{3/2}T^{3/2},$$

with

$$B_{3/2} = \frac{15\zeta(5/2)k_B^{5/2}}{32(\pi D_0)^{3/2}}.$$

The values of $B_{3/2}$ in the doping range $0.2<x<0.5$ are shown in Fig. 4 with $t=0.3$ eV (solid line) and $t=0.4$ eV (dotted line). The values of $B_{3/2}$ we obtained are close to the experimental data[31] ($B_{3/2}=1.1802$ mJ/$K^{5/2}$ mol for $x=0.2$ and $B_{3/2}=0.956\,72$ mJ/$K^{5/2}$ mol for $x=0.3$) if we use $t=0.4$ eV.

To sum up, the consistency of the magnitudes of γ and $B_{3/2}$ in the doping range $0.2<x<0.5$ evaluated in terms of the mean-field theory suggests that the low-temperature thermodynamics of the FM metallic phase can be well-described by the one-orbital QDE model, and this result can be viewed as an indirect evidence of spin-charge separation at low energy in the FM metallic phase.

D. Optical conductivity at low energy

One of the consequences of the spin-charge separation in our theory is that the optical conductivity at low frequency ($\omega \ll E_g$) is mainly contributed by free holons, where E_g denotes the gap of gauge fluctuations. Especially, the Drude weight is completely determined by free holons, which is given by

$$\mathcal{D} = -\frac{\pi e^2}{2l}K, \tag{27}$$

where K is the average kinetic energy of holons per site and $l \approx 3.9$ Å is the lattice constant. Following experiments, one may measure the Drude weight in unit of $\pi e^2/(2m_e l^3)$, denoted by DW, where m_e is the electron mass. Within our mean-field theory, DW at $T=0$ is

$$\mathrm{DW} = \frac{6m_e t l^2 \eta}{\hbar^2}\left(1-\frac{x}{4}\right), \tag{28}$$

where $\hbar$ is the Planck constant. The doping dependence for DW, given by Eq. (28), is shown in Fig. 5 with $t=0.3$ eV (solid line) and $t=0.2$ eV (dotted line). From it, we see that, in the doping range $0.2<x<0.5$, DW$\sim$0.19–0.26 for $t=0.3$ eV, and DW$\sim$0.13–0.18 for $t=0.2$ eV. Since the Drude peak at $T=0$ does not carry 100% of the weight, this result implies that some spectral weight must be transferred to higher energies ($\omega \geq E_g$) due to the optical conductivity sum rule, so that the Drude weight is suppressed compared with normal metals.

Optical conductivity spectra have been investigated for single crystals of $La_{1-x}Sr_xMnO_3$ with $0 \leq x \leq 0.3$.[13] The peculiar behaviors observed in the low-energy optical spectra ($\omega<0.1$ eV) in the FM metallic phase at low temperature, which cannot be explained by the simple Fermi-liquid picture, are as follows: (i) The low-energy spectra are composed mostly of the incoherent part and lightly of the Drude response (about 20%–30% in fraction). (ii) The Drude part is discernible below 0.04 eV, but with an anomalously small spectral weight. For example, the value of DW is as small as 0.012 even for the lowest temperature spectra for both $x=0.175$ and 0.3. Further optical studies on $La_{0.7}Ca_{0.3}MnO_3$ (Ref. 14) confirm that, in the FM metallic phase at very low temperatures, the low-energy optical conductivity spectra ($\omega<0.5$ eV) show two types of absorption features: a sharp Drude peak with little weight (about 33% in fraction or

DW ~ 0.02) superimposed to the broad incoherent absorption band. Our analysis indicates that in the FM metallic phase the optical conductivity spectra of the QDE model at low energy ($\omega \ll J_H$) indeed consists of two parts,

$$\sigma_1(\omega) \sim \sigma_c(\omega) + \sigma_{\text{inc}}(\omega),$$

where $\sigma_c(\omega)$ is the coherent (Drude) part, which is mainly contributed by holons, and $\sigma_{\text{inc}}(\omega)$ represents the incoherent part with most of its weight in the region $\omega \geqslant E_g$, which arises from the strong scattering between gauge fields and holons. Thus, according to our theory, the energy scale below which the Drude part is discernible can be regarded as the lower bound of E_g. A rough estimate of the value of E_g ($E_g \sim 0.038-0.071$ eV in the doping range $0.15 < x < 0.5$ for $t \sim 0.3$ eV) is consistent with the experiment. (See Sec. IV.) This picture is consistent with the observed optical spectra at low energy. However, the values of DW we obtained are larger than the experimental data by an order of magnitude. Since our mean-field theory is supposed to be accurate at low energy, the quantitative discrepancy between our results and the experimental data indicates that to explain the optical spectra of manganites, other ingredients beyond the one-orbital QDE model must be taken into account. Some possible scenarios, such as orbital fluctuations[32] or electron-phonon conplings,[33,34] have been proposed. Applying our method to these "extended" QDE models is an interesting problem.

E. The electron spectral function and tunneling density of states

The most important result in our mean-field theory is the spin-charge separation at low energy. A direct examination of this phenomenon is to study the behavior of the electron spectral function at low temperatures, which can be measured by the ARPES experiments. The electron spectral function is defined as

$$A(\omega,\boldsymbol{q}) \equiv -2\,\text{Im}\{\mathcal{G}(i\omega_n \to \omega,\boldsymbol{k})\}. \tag{29}$$

Here Im$\{\cdots\}$ means the imaginary part of $\cdots$, and $\mathcal{G}(K)$ with $K=(i\omega_n,\boldsymbol{k})$ is the Fourier transform of the electron Green function, which is defined by

$$\mathcal{G}(X) \equiv -\langle \mathcal{T}\{\bar{c}_{i\sigma}(\tau)\bar{c}^{\dagger}_{j\sigma}(0)\}\rangle = -\frac{1}{2S}\langle \mathcal{T}\{f^{\dagger}_{\boldsymbol{i}}(\tau)d_{i\sigma}(\tau)d^{\dagger}_{j\sigma}(0)f_{\boldsymbol{j}}(0)\}\rangle, \tag{30}$$

where $X=(\tau,\boldsymbol{i}-\boldsymbol{j})$.

At the mean-field level, holons and magnons are decoupled from one another and $d_{i\uparrow}$ is treated as a c number, instead of an operator. As a result, the electron Green function can be approximated as

$$\begin{aligned}\mathcal{G}(X) &\approx \frac{1}{2S}\langle \mathcal{T}\{f_{\boldsymbol{j}}(0)f^{\dagger}_{\boldsymbol{i}}(\tau)\}\rangle\langle d^{\dagger}_{i\uparrow}d_{i\uparrow}\rangle \\ &\quad + \frac{1}{2S}\langle \mathcal{T}\{f_{\boldsymbol{j}}(0)f^{\dagger}_{\boldsymbol{i}}(\tau)\}\rangle\langle \mathcal{T}\{d_{i\downarrow}(\tau)d^{\dagger}_{j\downarrow}(0)\}\rangle \\ &= -\frac{x_d(T)}{2S}G(-X) + \frac{1}{2S}G(-X)S(X),\end{aligned} \tag{31}$$

where $x_d(T)$ is determined by the equation

$$x_d(T) + \frac{1}{N}\sum_{\boldsymbol{k}} n_B(\omega_{\boldsymbol{k}}) = 2S - x, \tag{32}$$

and

$$G(X) = -\langle \mathcal{T}\{f_{\boldsymbol{i}}(\tau)f^{\dagger}_{\boldsymbol{j}}(0)\}\rangle,$$

$$S(X) = -\langle \mathcal{T}\{b_{\boldsymbol{i}}(\tau)b^{\dagger}_{\boldsymbol{j}}(0)\}\rangle,$$

are the propagators of holons and magnons, respectively. In terms of Eq. (31), the electron spectral function is given by[35]

$$A(\omega,\boldsymbol{k}) = Z(x,T)\,\delta(\omega + \epsilon_{\boldsymbol{k}} - \mu_f) + a(\omega,\boldsymbol{k}), \tag{33}$$

where $Z(x,T)=\pi x_d(T)/S$ and

$$a(\omega,\boldsymbol{k}) = \frac{\pi}{SN}\sum_{\boldsymbol{q}}[n_B(\omega_{\boldsymbol{k+q}}) + n_F(\epsilon_{\boldsymbol{q}} - \mu_f)] \times \delta(\omega + \epsilon_{\boldsymbol{q}} - \mu_f - \omega_{\boldsymbol{k+q}}).$$

Equation (33) indicates that the electron spectral function at low energy consists of two parts: a sharp quasiparticle peak, following the holon dispersion, superimposed to a broad incoherent part given by $a(\omega,\boldsymbol{k})$. The spectral weight of the quasiparticle peak is given by $Z(x,T)$, which is associated with the condensate of the d bosons. At $T \ll T_c$, it is given by

$$Z(x,T) \approx 2\pi\left[1 - \frac{x}{4} - \frac{\zeta(3/2)}{4}\left(\frac{Tl^2}{4\pi D_0}\right)^{3/2}\right]. \tag{34}$$

By taking into account impurity scattering and the interactions between holons and magnons, the δ-function peak will be broadened, and the width $1/\tau$ is given by $1/\tau = \max\{1/\tau_0, k_B T\}$ where τ_0 is the lifetime due to impurity scattering. The low-temperature behavior of $a(\omega,\boldsymbol{k}_F)$ at the hole concentration $x=0.4$ is shown in Fig. 6, where $\boldsymbol{k}_F \approx 0.74\pi(1,1,0)$ and $0.54\pi(1,1,1)$ in Figs. 6(a) and 6(b), respectively. Figure 7 shows $a(\omega,\boldsymbol{k})$ along the direction from $[0,0,0]$ to $[\pi,\pi,0]$, at the temperature $T/t=1/174$ and the hole concentration (a) $x=0.4$ and (b) $x=0.3$. A common feature of $a(\omega,\boldsymbol{k})$ is that it exhibits a broad asymmetric peak at low temperature with the width $\sim t$, and the peak position is at $\omega \sim 0.5t$ and $0.21t$ for $x=0.4$ and 0.3, respectively. Furthermore, at low temperature, the peak position and its width are insensitive to the variations of temperatures. This asymmetric peak implies the violation of the particle-hole symmetry. As raising the temperature, we can see a transfer of the spectral weight from the quasiparticle peak to the incoherent part. Such a trend persists until at the critical temperature where the coherent part disappears completely, i.e., $Z(x,T_c)=0$. The

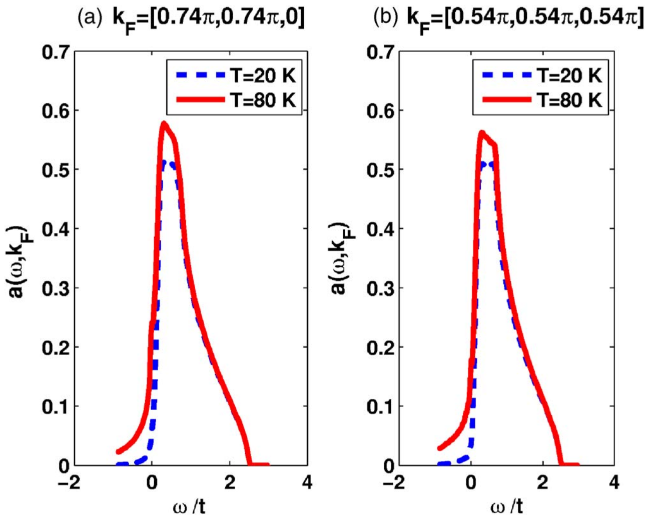

FIG. 6. (Color online) The electron spectral function, with the subtraction of the quasiparticle peak, at the hole concentration $x=0.4$. $\boldsymbol{k}_F$ denotes the Fermi momentum. The temperatures we consider are $T/t=1/174$ (dashed line) and $25/1088$ (solid line), which correspond to $T=20,80$ K, respectively, for $t=0.3$ eV.

presence of such a broad asymmetric peak at low temperature reflects the composite nature of electrons at low energy in the large U, J_H limit, i.e., a manifestation of the spin-charge separation at low energy, which can be observed in the photoemission experiment.

A similar form for the electron spectral function [Eq. (33)] was also obtained by a mean-field approximation to the DE model in the limit $J_H/t \to +\infty$.[9] There, the FM phase also corresponds to the condensed phase of the Schwinger bosons. However, the doping dependence of the mean-field parameters in that approach is different from ours, especially the bandwidth of holons. This results in distinct doping dependence for various physical quantities, such as the spin stiffness at $T=0$ and the Drude weight. Moreover, quadratic approximations for the dispersion relations of holons and magnons were used to calculate the electron spectral function, which leads to a weak logarithmic singularity in the incoherent part $a(\omega,\boldsymbol{k})$ with the width being of the order of the maximum magnon energy. We do not see such a singularity, as can be seen in Figs. 6 and 7. Further, the width of the broad peak we obtained is much larger, which is consistent with the ARPES measurements.

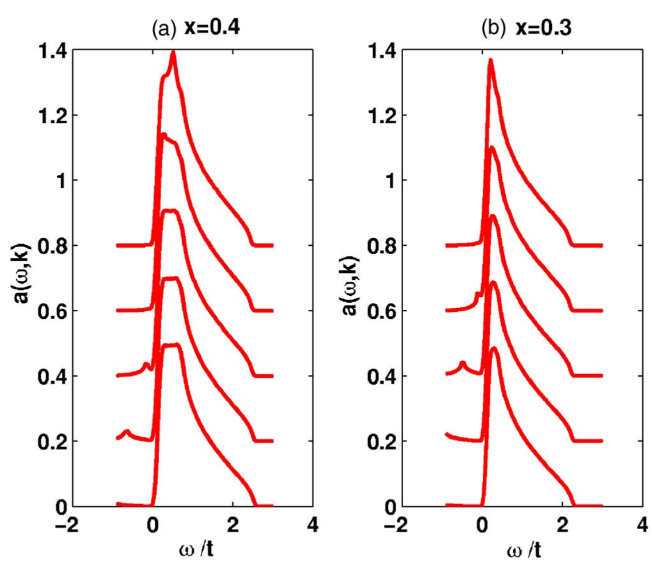

FIG. 7. (Color online) The electron spectral function, with the subtraction of the quasiparticle peak, at the temperature $T/t=1/174$ and hole concentration (a) $x=0.4$ and (b) $x=0.3$. Here $\boldsymbol{k}=k_0\times[\pi,\pi,0]$ with $k_0=0.5,0.6,0.7,0.8,0.9$ from bottom to top.

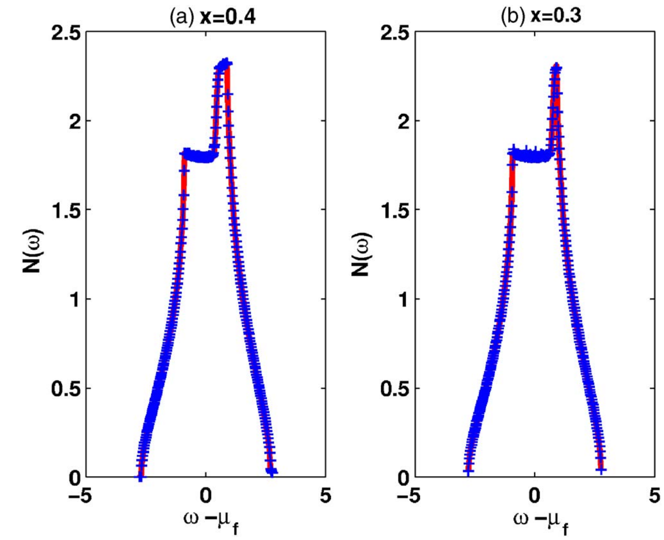

FIG. 8. (Color online) The tunneling DOS at the temperatures $T/t=1/174$ (solid line) and $25/1088$ (+) with the hole concentration (a) $x=0.4$ and (b) $x=0.3$. We have set $t=1$.

Another quantity which is related to $A(\omega,\boldsymbol{k})$ is the tunneling DOS,

$$N(\omega) = \frac{1}{N}\sum_{\boldsymbol{k}} A(\omega,\boldsymbol{k}) \tag{35}$$

which can be measured by the scanning tunneling spectroscopy (STS). Within the mean-field theory, $N(\omega)$ can be written as

$$N(\omega) = \frac{Z(x,T)}{t(1-x/4)} N_3\left(\frac{\bar{\omega}}{1-x/4}\right) + \frac{1}{N}\sum_{\boldsymbol{k}} a(\omega,\boldsymbol{k}), \tag{36}$$

where $N_3(\epsilon) \equiv \frac{1}{N}\sum_{\boldsymbol{k}} \delta[\epsilon - \sum_{\boldsymbol{u}} \cos(\boldsymbol{k}\cdot\boldsymbol{u})]$ and $\bar{\omega}=(\omega-\mu_f)/t$. Figure 8 shows $N(\omega)$ as a function of $\bar{\omega}$ at two temperatures $T/t=1/174$ and $25/1088$ with the hole concentration (a) $x=0.4$ and (b) $x=0.3$. A few salient features about the low-temperature behavior of the tunneling DOS are as follows: (i) $N(\omega)$ consists of two parts: One is proportional to the DOS for a tight-binding model on a simple cubic lattice, which is contributed by the quasiparticle peak of the electron spectral function, and the other exhibits an asymmetric peak, which results from the incoherent part of the electron spectral function. (ii) The position of the asymmetric peak is at $\omega-\mu_f \sim \chi(T=0)t$, the renormalized hopping amplitude of holons. (iii) The value of $N(\omega)$ is insensitive to the variation of temperatures. Again, this structure of $N(\omega)$ is a natural consequence of spin-charge separation.

Variable temperature STS studies on single crystals of $La_{0.7}Pb_{0.3}MnO_3$ have been done in the temperature range 100–375 K.[36] Experimental data show that $N(\epsilon_F)$ grows rapidly below T_c and reaches a temperature independent value, where ϵ_F is the Fermi energy. Furthermore, $N(\omega)$ near ϵ_F is flat in the scale of T below T_c. Further STS studies on single crystals of $La_{0.7}Ca_{0.3}MnO_3$ (Ref. 37) confirm these results. Our prediction about the behavior of $N(\omega)$ near the Fermi energy is consistent with experimental results. Further STS studies at low temperatures must be performed to verify our mean-field theory. Especially, an observation of the asymmetric peak away from the Fermi energy in the tunneling DOS at low temperatures will be solid confirmation of the slave-fermion theory.

IV. GAUGE FLUCTUATIONS AND THE STABILITY OF THE MEAN-FIELD STATE

In order to study the role of gauge fluctuations and to derive the low-energy effective theory, we can start with Eq. (9), and parametrize the Hubbard-Stratonovich fields as

$$\chi_{i+u,i} = \chi e^{-i\phi_{i,u}}, \quad \eta_{i+u,i} = \eta e^{-i\tilde{\phi}_{i,u}}. \tag{37}$$

One may further decompose $\phi_{i,u}$ and $\tilde{\phi}_{i,u}$ by

$$\phi_{i,u} = \mathcal{A}_{i,u} + \mathcal{B}_{i,u}, \quad \tilde{\phi}_{i,u} = \mathcal{A}_{i,u} - \mathcal{B}_{i,u}. \tag{38}$$

Such a decomposition becomes transparent once we realize that under the U(1) gauge transformation, $\mathcal{A}_{i,u}$ transforms like a gauge field, while $\mathcal{B}_{i,u}$ is gauge invariant. Simple manipulations show that the $\mathcal{B}_{i,u}$ field acquires a finite energy gap. Furthermore, the amplitude fluctuations of $\chi_{i+u,i}$ and $\eta_{i+u,i}$ are also gapped. For the energy below these mass gaps, one may integrate out the massive fields and take the continuum limit

$$f_i \to l^{d/2} h(X), \quad d_{i\sigma} \to l^{d/2} d_\sigma(X),$$

$$\mathcal{A}_{i,u} \to \boldsymbol{u}\cdot\boldsymbol{a}(X), \quad \lambda_i \to \lambda(X), \tag{39}$$

where $X=(\tau,\boldsymbol{x})$. After doing so, we arrive at the following continuum Lagrangian within the effective-mass approximation

$$\mathcal{L} = \sum_\sigma d_\sigma^\dagger(\partial_\tau + i\lambda)d_\sigma + h^\dagger(\partial_\tau + i\lambda - \mu_0)h - 2iM\lambda + \frac{1}{2m_f}|(\boldsymbol{\nabla} - i\boldsymbol{a})h|^2 + \sum_\sigma \frac{1}{2m_b}|(\boldsymbol{\nabla} - i\boldsymbol{a})d_\sigma|^2, \tag{40}$$

where $M=Sl^{-3}$. In view of Eq. (40), the Lagrangian multiplier λ plays the role of the time component of the gauge fields.

In the FM phase, without loss of generality, one may parametrize d_σ in the following way:

$$d_\uparrow = \sqrt{n_d + \rho}\, e^{i\phi}, \quad d_\downarrow = b, \tag{41}$$

on account of the BEC of the Schwinger bosons, where $n_d = (2S-x)l^{-3}$ is the average density of d bosons, and ρ and ϕ describe the amplitude and phase fluctuations of $d_\uparrow$, respectively. That is, we choose the direction of the order parameter (magnetization) to be the z axis. Inserting Eq. (41) into Eq. (40) gives rise to

$$\mathcal{L}_{\rm FM} = b^\dagger(\partial_\tau + i\lambda)b + h^\dagger(\partial_\tau + i\lambda - \mu_0)h - in\lambda + \frac{1}{2m_f}|(\boldsymbol{\nabla} - i\boldsymbol{a})h|^2 + \frac{1}{2m_b}|(\boldsymbol{\nabla} - i\boldsymbol{a})b|^2 + \frac{1}{8m_b n_d}|\boldsymbol{\nabla}\rho|^2 + \frac{n_d}{2m_b}|\boldsymbol{\nabla}\phi - \boldsymbol{a}|^2 + \frac{1}{2m_b}\rho|\boldsymbol{\nabla}\phi - \boldsymbol{a}|^2 + i\rho(\lambda + \partial_\tau\phi).$$

The U(1) gauge structure of $\mathcal{L}_{\rm FM}$ now reads

$$h \to he^{-iw}, \quad b \to be^{-iw},$$

$$\rho \to \rho, \quad \phi \to \phi - w,$$

$$\boldsymbol{a} \to \boldsymbol{a} - \boldsymbol{\nabla}w, \quad \lambda \to \lambda + \partial_\tau w. \tag{42}$$

With an eye on the gauge invariance of $\mathcal{L}_{\rm FM}$, one may choose the gauge $w=\phi$. This amounts to redefining the h, b, $\boldsymbol{a}$, and λ as follows:

$$\tilde{h} = he^{-i\phi}, \quad \tilde{b} = be^{-i\phi},$$

$$\tilde{\boldsymbol{a}} = \boldsymbol{a} - \boldsymbol{\nabla}\phi, \quad \tilde{\lambda} = \lambda + \partial_\tau\phi. \tag{43}$$

We notice that $\tilde{h}$, $\tilde{b}$, $\tilde{\boldsymbol{a}}$, and $\tilde{\lambda}$ are all gauge invariant. In terms of Eq. (43), $\mathcal{L}_{\rm FM}$ becomes

$$\mathcal{L}_{\rm FM} = \tilde{b}^\dagger(\partial_\tau + i\tilde{\lambda})\tilde{b} + \tilde{h}^\dagger(\partial_\tau + i\tilde{\lambda} - \mu_0)\tilde{h} + i(\rho - n)\tilde{\lambda} + \frac{1}{2m_f}|(\boldsymbol{\nabla} - i\tilde{\boldsymbol{a}})\tilde{h}|^2 + \frac{1}{2m_b}|(\boldsymbol{\nabla} - i\tilde{\boldsymbol{a}})\tilde{b}|^2 + \frac{1}{8m_b n_d}|\boldsymbol{\nabla}\rho|^2 + \frac{1}{2m_b}(n_d + \rho)\tilde{\boldsymbol{a}}^2.$$

In the above, the higher order terms in ρ, i.e., the self-interactions of ρ, have been neglected. This is because they only generate irrelevant operators. Integrating out $\tilde{\lambda}$ gives rise to the constraint

$$\tilde{b}^\dagger\tilde{b} + \tilde{h}^\dagger\tilde{h} + \rho = n, \tag{44}$$

which is nothing but the continuum version of the NDO condition [Eq. (7)]. Using Eq. (44), one may further integrate out the ρ field, yielding

$$\mathcal{L}_{\rm FM} = \tilde{h}^\dagger(\partial_\tau - \mu_0)\tilde{h} + \frac{1}{2m_f}|\boldsymbol{\nabla}\tilde{h}|^2 + \tilde{b}^\dagger\partial_\tau\tilde{b} + D_0|\boldsymbol{\nabla}\tilde{b}|^2 + \frac{1}{2}m_a\tilde{\boldsymbol{a}}^2 + \cdots,$$

where $\cdots$ represents the interactions between $\tilde{h}$, $\tilde{b}$, and $\tilde{\boldsymbol{a}}$, $D_0=(2m_b)^{-1}$ is the FM spin stiffness at $T=0$, and $m_a=[2M-(1-m_b/m_f)n]/m_b$.

We see that in the FM phase the gauge fields acquire a "mass" term through the Anderson-Higgs mechanism. In other words, the excitations corresponding to $\tilde{\boldsymbol{a}}$ acquire a finite energy gap $E_g \sim m_a/k_F$, up to a multiplicative constant of order one, where k_F is the Fermi momentum of holons. Using the mean-field parameters, m_f can be estimated as $m_f^{-1}=(1-x/4)tl^2$, and we have

$$\frac{E_g}{t} \sim \frac{4\sqrt{2}D_0/(tl^2)}{\sqrt{3+W/f(x)}}\left\{1-\frac{x}{4}\left[1-f(x)\left(\frac{tl^2}{2D_0}\right)\right]\right\}, \quad (45)$$

where $W=\epsilon_F/t$ and $f(x)=1-x/4$. Equation (45) gives rise to the values $E_g/t=0.1273-0.2381$ in the doping range $0.15<x<0.5$. For $t\sim 0.3$ eV, this corresponds to $E_g \sim 0.038-0.071$ eV, which is about the same order of T_c.

When the energy is much lower than E_g, one may further integrate out $\tilde{\boldsymbol{a}}$, the resulting effective Lagrangian can be written as $\mathcal{L}_{\mathrm{FM}}=\mathcal{L}_0+\mathcal{L}_{\mathrm{int}}$ where

$$\mathcal{L}_0=\tilde{h}^\dagger(\partial_\tau-\mu_f)\tilde{h}+\frac{1}{2m_f}|\nabla\tilde{h}|^2+\tilde{b}^\dagger\partial_\tau\tilde{b}+D_0|\nabla\tilde{b}|^2 \quad (46)$$

and

$$\mathcal{L}_{\mathrm{int}}=\frac{g_1}{2}(\boldsymbol{j}_h+\boldsymbol{j}_b)^2+\frac{g_2}{2}(\nabla\rho_h+\nabla\rho_b)^2. \quad (47)$$

In Eq. (47), we only keep the most relevant operators around the FM fixed point, described by $\mathcal{L}_0$, in the sense of RG, and $\boldsymbol{j}_h(\boldsymbol{j}_b)$ and $\rho_h(\rho_b)$ are the current and density operators for the $\tilde{h}(\tilde{b})$ fields, respectively.

Since $\mathcal{L}_{\mathrm{int}}$ is irrelevant around the fixed point described by $\mathcal{L}_0$, our low-energy effective theory shows clearly that the FM phase of the QDE model exhibits the phenomenon of spin-charge separation. That is, the low-energy excitations are holons described by the $\tilde{h}$ field, which carry charge e and spin zero, and the FM spin waves (magnons) described by the $\tilde{b}$ field, which are charge neutral and carry spin-1. This is very different from the usual itinerant ferromagnets, where the elementary excitations are the dressed electrons, which carry charge $-e$ and spin-1/2, and the magnons, which are collective excitations in the particle-hole channel.

V. CONCLUSION AND DISCUSSIONS

To summarize, we have studied the low-energy physics of the QDE model based on the slave-fermion formulation. The most important feature of this approach is that the effects of large values of U and J_H are taken into account right from the beginning. (For the one-orbital model, the large U, J_H limit is implemented by the NDO condition.) This results in a non-Fermi-liquid ground state, in contrast to most of the previous studies on the DE model. A direct consequence following it is that the electron spectral function exhibits a broad asymmetric peak away from the Fermi surface, in addition to the quasiparticle peak. Both our results about the low-energy magnetic properties and low-temperature thermodynamics are also consistent with experimental data in the FM metallic phase. On the other hand, our prediction for the optical conductivity at low energy is only qualitatively consistent with experiments. Quantitatively, the Drude weight we obtained is larger than that actually observed. This indicates that to have a good quantitative description for the low-frequency optical spectra of manganties, some extra ingredients beyond the one-orbital QDE model must be taken into account. However, we should emphasize that, for such a scenario to be valid, the inclusion of these new ingredients should not affect the low-temperature thermodynamics and low-energy magnetic properties predicted by the one-orbital QDE model in any drastic way because the one-orbital model already gives rise to reasonable results on them.

We have also studied the role of gauge fluctuations and derived a low-energy continuum effective theory. A previous study in terms of the slave-fermion gauge theory claimed that the gapless *longitudinal* gauge fluctuations play a dominant role on the electronic spectral properties.[20] However, the longitudinal component of gauge fields is gauge dependent and physics should be independent of the gauge choice. Moreover, both the time and longitudinal components of gauge fields are screened in the metallic phase, which cannot affect low-energy physics dramatically. What we do in Sec. IV is to explicitly show that the gauge fluctuations in the FM phase, both the transverse and longitudinal components, are completely screened due to the Anderson-Higgs mechanism. The resulting electron spectral function in the FM metallic phase consists of two parts: one the sharp quasiparticle peak at the Fermi energy and the other an asymmetric broad peak away from the Fermi energy, instead of a broad quasiparticle peak at the Fermi energy. These predictions can be observed from the ARPES or STS measurements.

From the theoretical point of view, the slave-fermion formulation also gives a clear picture of the apparently observed Fermi-liquid behavior and its possible deviations. Within this framework, the Fermi-liquid-like behaviors, such as a small value of the Drude weight in the optical spectra and a small coherent quasiparticle peak in the electron spectral function, are consequences of the Bose condensation of the spinon field. Therefore, the spectral weight is directly related to the magnitude of the condensate. Based on the similar reasoning, we expect that in low dimensional or layered materials where the quantum fluctuations tend to kill the Bose condensate, the coherent quasiparticle peak will either disappear completely or be greatly reduced in comparison with the three-dimensional results we obtained here.[28,38] This is actually observed in the ARPES measurements for layered compounds.[15,16] Another minimal extension of the one-orbital QDE model, which has the potential to reduce the quasiparticle peak or the Drude weight, is to include the orbital degrees of freedom. In this case, we have two slave boson fields: one describing the spin fluctuations and the other describing the orbital fluctuations. If only the spin slave field condenses at low temperature, the strong orbital fluctuations will also tend to reduce the coherent parts in the optical conductivity and the electron spectral function. Researches along these directions are in progress.

ACKNOWLEDGMENTS

The authors would like to thank C.-D. Hu for introducing Refs. 10 and 19. The authors are also grateful to the hospitality of National Center for Theoretical Sciences (North), where this work was initiated. The work of one of the authors (Y.L.L.) is supported by the National Science Council of Taiwan under Grant No. NSC 95-2112-M-018-008. The work of one of the authors (Y.-W.L.) is supported by the National Science Council of Taiwan under Grant No. NSC 95-2112-M-029-009.

[1] P. Schiffer, A. P. Ramirez, W. Bao, and S.-W. Cheong, Phys. Rev. Lett. **75**, 3336 (1995).

[2] E. Dagotto, *Nanoscale Phase Separation and Colossal Magnetoresistance* (Springer-Verlag, Berlin, 2003) and references therein.

[3] C. Zener, Phys. Rev. **82**, 403 (1951).

[4] P. W. Anderson and H. Hasegawa, Phys. Rev. **100**, 675 (1955).

[5] P.-G. de Gennes, Phys. Rev. **118**, 141 (1960).

[6] K. Kubo and N. Ohata, J. Phys. Soc. Jpn. **33**, 21 (1972).

[7] N. Furukawa, J. Phys. Soc. Jpn. **65**, 1174 (1996).

[8] S. Satpathy, Z. S. Popović, and F. R. Vukajlović, Phys. Rev. Lett. **76**, 960 (1996); J. E. Medvedeva, V. I. Anisimov, O. N. Mryasov, and A. J. Freeman, J. Phys.: Condens. Matter **14**, 4533 (2002).

[9] S. K. Sarkar, J. Phys.: Condens. Matter **8**, L515 (1996).

[10] G. Khaliullin and R. Kilian, Phys. Rev. B **61**, 3494 (2000).

[11] D. I. Golosov, Phys. Rev. Lett. **84**, 3974 (2000).

[12] N. Shannon and A. V. Chubukov, Phys. Rev. B **65**, 104418 (2002).

[13] Y. Okimoto, T. Katsufuji, T. Ishikawa, T. Arima, and Y. Tokura, Phys. Rev. B **55**, 4206 (1997).

[14] K. H. Kim, J. H. Jung, and T. W. Noh, Phys. Rev. Lett. **81**, 1517 (1998).

[15] D. S. Dessau, T. Saitoh, C.-H. Park, Z.-X. Shen, P. Villella, N. Hamada, Y. Moritomo, and Y. Tokura, Phys. Rev. Lett. **81**, 192 (1998); T. Saitoh, D. S. Dessau, Y. Moritomo, T. Kimura, Y. Tokura, and N. Hamada, Phys. Rev. B **62**, 1039 (2000).

[16] Y.-D. Chuang, A. D. Gromko, D. S. Dessau, T. Kimura, and Y. Tokura, Science **292**, 1509 (2001).

[17] J.-H. Park, C. T. Chen, S-W. Cheong, W. Bao, G. Meigs, V. Chakarian, and Y. U. Idzerda, Phys. Rev. Lett. **76**, 4215 (1996); D. D. Sarma, N. Shanthi, S. R. Krishnakumar, T. Saitoh, T. Mizokawa, A. Sekiyama, K. Kobayashi, A. Fujimori, E. Weschke, R. Meier, G. Kaindl, Y. Takeda, and M. Takano, Phys. Rev. B **53**, 6873 (1996).

[18] D. I. Golosov, Phys. Rev. B **71**, 014428 (2005).

[19] A. Weiße, J. Loos, and H. Fehske, Phys. Rev. B **64**, 054406 (2001).

[20] C.-D. Hu, Phys. Rev. Lett. **93**, 157205 (2004).

[21] For detailed discussions about the slave-particle representation, one may consult, for example, A. Auerbach, *Interacting Electrons and Quantum Magnetism* (Springer-Verlag, New York, 1994); X. G. Wen, *Quantum Field Theory of Many-Body Systems* (Oxford University Press, New York, 2004).

[22] For the one-orbital model, the large J_H limit amounts to the large U limit, provided one can treat the NDO condition exactly. An intuitive arguement goes as follows: The large J_H limit forces the spins of the conduction electrons to be parallel to the core spins. In the FM phase, it follows that there can be no doubly occupied sites due to the Pauli exclusion principle. However, in our approach, we first impose the NDO condition by taking the $U/t \rightarrow +\infty$ limit. This, in our opinion, makes the introduction of Eq. (5) clearer and the derivation of our working Hamiltonian [Eq. (6)] smoother. Furthermore, this approach can be easily generalized to the slave-fermion formulation of the DE model with degenerate orbitals.

[23] J.-H. Park, E. Vescovo, H.-J. Kim, C. Kwon, R. Ramesh, and T. Venkatesan, Nature (London) **392**, 794 (1998).

[24] T. A. Kaplan and S. D. Mahanti, J. Phys.: Condens. Matter **9**, L291 (1997).

[25] T. G. Perring, G. Aeppli, S. M. Hayden, S. A. Carter, J. P. Remeika, and S.-W Cheong, Phys. Rev. Lett. **77**, 711 (1996).

[26] H. Y. Hwang, P. Dai, S.-W. Cheong, G. Aeppli, D. A. Tennant, and H. A. Mook, Phys. Rev. Lett. **80**, 1316 (1998); L. Vasiliu-Doloc, J. W. Lynn, A. H. Moudden, A. M. de Leon-Guevara, and A. Revcolevschi, Phys. Rev. B **58**, 14913 (1998); P. Dai, H. Y. Hwang, J. Zhang, J. A. Fernandez-Baca, S.-W. Cheong, C. Kloc, Y. Tomioka, and Y. Tokura, *ibid.* **61**, 9553 (2000).

[27] The spin-wave theory of the DE model indicates a "softening" of modes at the zone boundary for $x < 0.06$. See Ref. 12.

[28] T. A. Kaplan, S. D. Mahanti, and Y.-S. Su, Phys. Rev. Lett. **86**, 3634 (2001).

[29] For a lucid discussion on Landau damping in the Fermi liquids, see, for example, D. Pines and P. Nozières, *The Theory of Quantum Liquids* (Benjamin, New York, 1966), Vol. 1.

[30] G.-M. Zhao, K. Conder, H. Keller, and K. A. Müller, Nature (London) **381**, 676 (1996). See also I. Isaac and J. P. Franck, Phys. Rev. B **57**, R5602 (1998).

[31] B. F. Woodfield, M. L. Wilson, and J. M. Byers, Phys. Rev. Lett. **78**, 3201 (1997).

[32] F. Mack and P. Horsch, Phys. Rev. Lett. **82**, 3160 (1999); P. Horsch, J. Jaklič, and F. Mack, Phys. Rev. B **59**, 6217 (1999).

[33] A. J. Millis, R. Müller, and B. I. Shraiman, Phys. Rev. B **54**, 5405 (1996); S. Yunoki, A. Moreo, and E. Dagotto, Phys. Rev. Lett. **81**, 5612 (1998).

[34] For a review, see, for example, D. M. Edwards, Adv. Phys. **51**, 1259 (2002).

[35] We notice that in the QDE model, which is defined in a projected low energy Hilbert space, the electron spectral function satisfies the sum rule $\int_{-\infty}^{+\infty}\frac{dw}{2\pi}A(w,\boldsymbol{q})=1+x$ [Eq. (48)] due to the NDO condition. With the help of Eq. (32), one may verify that the mean-field result [Eq. (33)] *does not* satisfy the sum rule (48). Such a discrepancy is easily understood: the mean-field result does not include the higher energy ($\omega \geqslant E_g$) spectral weight which arises from the scattering between the holons and the *massive* gauge fields.

[36] A. Biswas, S. Elizabeth, A. K. Raychaudhuri, and H. L. Bhat, Phys. Rev. B **59**, 5368 (1999).

[37] M. Fäth, S. Freisem, A. A. Menovsky, Y. Tomioka, J. Aarts, and J. A. Mydosh, Science **285**, 1540 (1999).

[38] A. Moreo, S. Yunoki, and E. Dagotto, Phys. Rev. Lett. **83**, 2773 (1999).